rhd instruments
flexible cell solutions

Application note

Determination of the temperature-dependent ionic conductivity of ceramic solid electrolytes

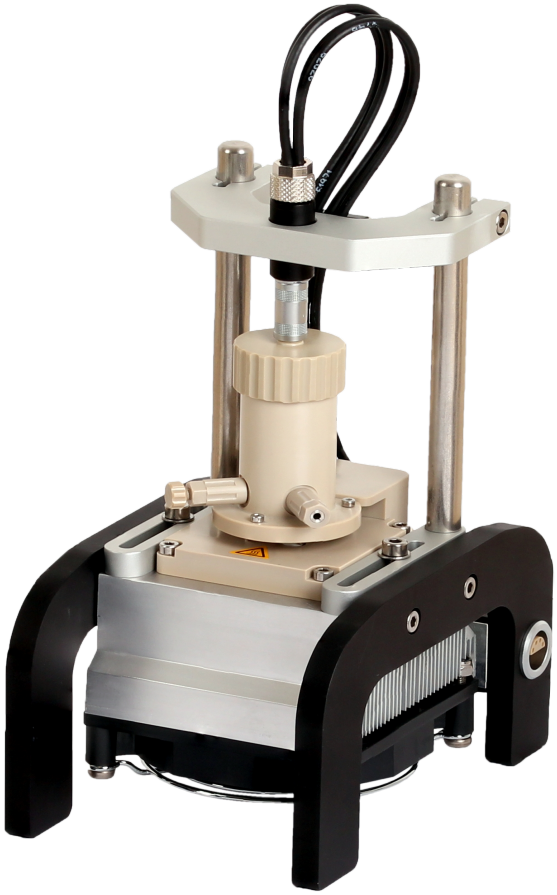

04/2021
rhd instruments GmbH & Co. KG

Introduction

With further progress in improving lithium ion batteries, the focus of research has turned to alternative technologies (next-generation batteries) like all-solid-state-batteries (ASSB), since these systems have the potential to exceed current battery systems in terms of energy density as well as safety concerns.[1]

For commercial use of ASSBs, it is crucial to use highly ionically conductive solid electrolytes while simultaneously ensuring proper interfacial contact and stability. During the last years, very promising solid electrolyte candidates based on oxide-type ceramics have been synthesized and investigated, showing ionic conductivities in the range of 0.1 to 1 mS cm^{-1} at room temperature.[2]-[3] Oxide ceramic based solid electrolytes were recently also used as component of hybrid electrolytes.[4]

Given this background, in this application note we want to focus on showing how to measure the temperature-dependent conductivity of a garnet-type $Li_7La_3Zr_2O_{12}$ (LLZO) sample by use of our Microcell HC system equipped with a TSC battery standard cell. The measurements were conducted in cooperation with the Fraunhofer Institute for Ceramic Technologies and Systems IKTS.

Experimental

a) Chemicals

For our investigations, we were provided with a LLZO pellet (d = 1.58 mm) by our partners at Fraunhofer Institute for Ceramic Technologies and Systems IKTS. The pellet was sputter-coated with a thin copper layer (Ø 9.5 mm) on both surfaces to ensure a proper electrical contact between the electrodes and the sample and hence a low contact resistance. The pellet was stored and handled under inert conditions (inert argon atmosphere inside of a glovebox).

b) Sample preparation & measuring setup

For the electrochemical measurements, a TSC battery standard cell, see **Figure 1**, in combination with a Microcell HC setup (rhd instruments GmbH & Co. KG) was used. As current collectors, two planar stainless steel disc electrodes press-fitted into a PEEK sleeve were used. For calculating the cell constant, the area of the copper layer on the pellet and the pellet thickness were used, resulting in a value of 0.223 cm^{-1}. The contact pressure applied onto the pellet inside of the TSC battery cell was adjusted to approximately 81 kPa using a gold-plated spring with a spring constant of 2.43 N mm^{-1}.

In the Microcell HC setup, the temperature is adjusted via a Peltier element. The accessible temperature range is -40 °C to +100 °C. For measuring the temperature, a Pt100 temperature sensor is embedded in the base unit of the TSC battery cell, at a position very close to the sample. The accuracy of the temperature is 0.1 °C with regard to the base unit.

Because the TSC battery measuring cell is completely airtight, the experiments took place on the Microcell system outside of the glove box.

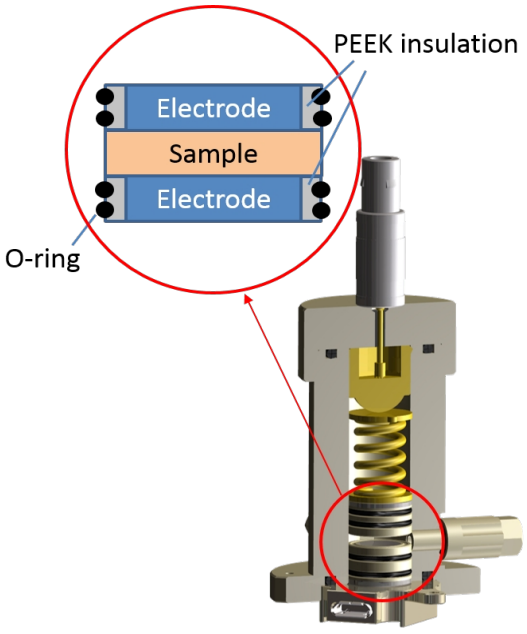

Figure 1: Schematic drawing of the measuring cell TSC battery standard. The sample pellet is placed between the upper and lower electrode. Both contact surfaces of the sample had been sputter-coated with a thin copper layer to ensure a good electrical contact.

For the impedance measurements, a Metrohm Autolab PGSTAT204 equipped with a FRA32-module was used. The communication with the temperature controller is integrated in the NOVA 2.1.5 software enabling automated measuring routines.

The recorded impedance data were evaluated by equivalent circuit fitting using the impedance data analysis software RelaxIS 3 (rhd instruments GmbH & Co. KG).

c) Measurement parameters

The impedance measurements were performed at a frequency range of 1 MHz to 0.1 Hz with an amplitude of $V_{AC,rms} = 10.0$ mV.

After reaching a temperature set point, a waiting time of 900 s was chosen followed by a OCP measurement for 3600 s to ensure for complete thermal equilibrium.

The measurement was performed at temperatures ranging from +30 °C down to -10 °C in steps of 10 °C.

Step	Action to be performed
1	Taking the prepared cell out of the glove box and connecting it to the Microcell HC cell stand.
2	Connecting the measuring device (2-electrode configuration).
3	Setting temperature to the first value and waiting until the set-point has been reached.
4	Waiting for 900 s and then measuring the OCP for 3600 s.
5	Performing an impedance spectroscopy measurement.
6	After finishing step 5, repeat steps 3 to 5 for every temperature value.

Results

The resulting impedance spectra for the different temperatures are shown in **Figure 2.**

For lower temperatures, the existence of two bulk processes is clearly visible: at high frequencies, a first semi-circle caused by ion transport inside of the grains is followed by another semi-circle in the mid-frequency range attributed to grain-boundary ion transport. At low frequencies, electrode polarisation and interfacial processes dominate.

As expected, the overall spectrum is shifted towards higher impedance values along the *Z'*-axis with decreasing temperature due to the temperature-induced decrease of overall conductivity.

The spectra were fitted with the equivalent circuit shown in **Figure 3**. Two serially connected parallel *R*/*CPE*-elements represent the resistance to ion migration and the related parallel bulk capacitance of grain (R_g/CPE_g) and grain-boundary processes (R_{gb}/CPE_{gb}), while some further CPE_{int}-element is needed to describe the low-frequency processes taking place at the electrode-sample interface.

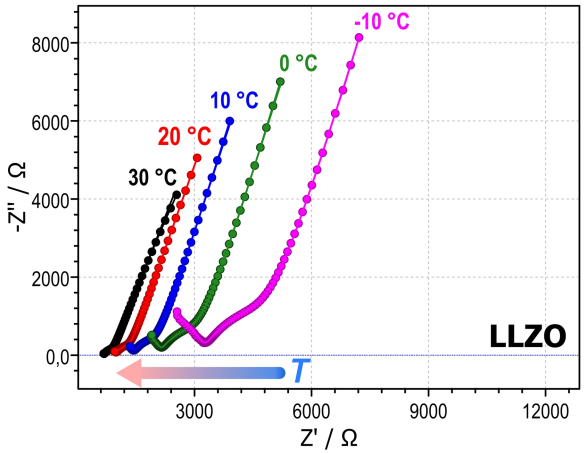

Figure 2: Temperature-dependent impedance spectra for the LLZO pellet. For a better visibility of the bulk-related features, the spectra were cut at 100 Hz.

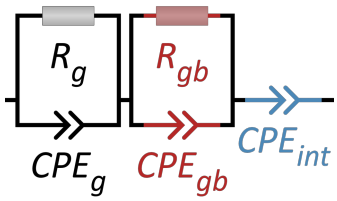

Figure 3: Equivalent circuits for fitting the impedance spectra.

Taking into account the sample thickness *d*, the area *A* of the sputtered copper electrode and the sum of the fitted resistance values R_g and R_{gb}, the corresponding total ionic conduct-

ivity σ_{total} as well as grain conductivity σ_g can be calculated as shown below.

$$\sigma_{total} = \frac{1}{R_g + R_{gb}} \cdot \frac{d}{A}$$

$$\sigma_g = \frac{1}{R_g} \cdot \frac{d}{A}$$

The resulting temperature-dependent ionic conductivity values are given in the following table.

T / °C	σ_{total} / 10^{-4} S cm^{-1}	σ_g / 10^{-4} S cm^{-1}
-10	0.47	0.69
0	0.73	1.04
10	1.13	1.54
20	1.71	2.24
30	2.57	3.19

A linearised Arrhenius-type evaluation was performed for both the temperature-dependent grain conductivity and total ionic conductivity values. Linear regression results in an activation barrier of $E_{A,\sigma g}$ = 0.29 eV for the grain conductivity and $E_{A,\sigma total}$ = 0.32 eV for the total ionic conductivity (**Figure 4**).

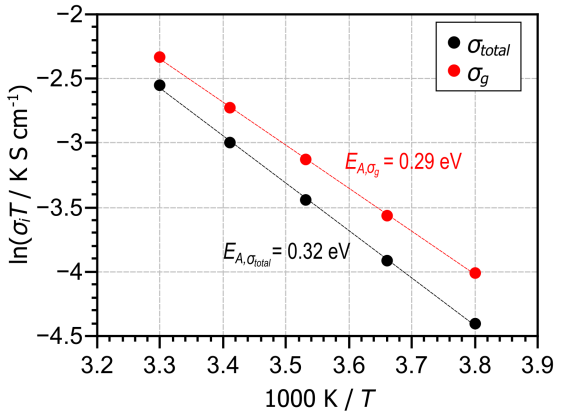

Figure 4: Arrhenius-plot and fit curves for the calculated total ionic conductivity (●) and grain conductivity (●) values of the sample pellet.

The conductivity values as well as the activation energy for the ionic conductivity are comparable to values reported in literature.[3]-[5]

Summary

In this application note we demonstrated how to determine the temperature-dependent ionic conductivity of a LLZO pellet by using a Microcell HC setup combined with a TSC battery standard cell.

Being able to perform those experiments with such turn-key-system and automated procedures allows for three things at once: Saving valuable time, optimised user-friendliness and reproducible measurement conditions.

Acknowledgement

We kindly acknowledge Juliane Hüttl, Arno Görne and Michael Arnold (Fraunhofer Institute for Ceramic Technologies and Systems IKTS) for sample preparation and highly appreciate the inspiring and fruitful discussions.

Literature

[1] Y. Chen, K. Wen, T. Chen, X. Zhang, M. Armand, S. Chen, *Energy Stor. Mater.* **2020**, *31*, 401-433.

[2] H.-Y. Li, B. Huang, Z. Huang, C.-A. Wang, *Ceramics International.* **2019**, *45*, 18115-18118.

[3] C. Shao, H. Liu, Z. Yu, Z. Zheng, N. Sun, C. Diao, *Solid State Ionics* **2016**, *287*, 13-16.

[4] M. Wirtz, M. Linhorst, P. Veelken, H. Tempel, H. Kungl, B. M. Moerschbacher, R.-A. Eichel, *Electrochem. Sci. Adv.* **2020**, e20000029.

[5] V. Thangadurai, S. Narayanan, D. Pinzaru, *Chem. Soc. Rev.* **2014**, *43*, 4714-4727.